

# Ultra-robust Metallosupramolecular Hydrogels with Unprecedented Self-recoverability Using Asymmetrically Distributed Carboxyl-Fe<sup>3+</sup> Coordination Interactions

Zhao-Yang Yuan, Zhen-Xing Cao, Rui Wu, Hui Li, Qiong-Jun Xu, Hai-Tao Wu, Jing Zheng\*, and Jin-Rong Wu\*

State Key Laboratory of Polymer Materials Engineering, College of Polymer Science and Engineering, Sichuan University, Chengdu 610065, China

 Electronic Supplementary Information

**Abstract** Recently, numerous mechanically robust synthetic hydrogels have been created. However, unlike natural load-bearing materials such as cartilages and muscles, most hydrogels have inherently contradictory requirements, obstructing the design of hydrogels with characteristics of robustness and rapid self-recoverability. Herein, we present a facile strategy for constructing mechanically robust and rapidly self-recoverable hydrogels. The linear poly(acrylamide-co-itaconic acid) chains crosslink *via* coordination bonds and minimal chemical crosslinkers to form the hydrogel network. Such design endows the coordination interactions to be asymmetrically distributed. Under deformation, the coordination interactions exhibit a reversible dissociation-and-reorganization property, demonstrating a new mechanism for energy dissipation and stress redistribution. Thus, the hydrogels possess tensile strength up to 12.5 MPa and toughness up to 28.2 MJ/m<sup>3</sup>. Moreover, the inherent dynamic nature of the coordination bonds imparts these hydrogels with stretch rate- and temperature-dependent mechanical behavior as well as excellent self-recovery performance. The method employed in this study is universal and is applicable to other polymers with load-bearing yet rapid recovery conditions. This study will facilitate diverse applications of most metallosupramolecular hydrogels.

**Keywords** Metallosupramolecular hydrogels; Coordination interactions; Self-recoverability

**Citation:** Yuan, Z. Y.; Cao, Z. X.; Wu, R.; Li, H.; Xu, Q. J.; Wu, H. T.; Zheng, J.; Wu, J. R. Ultra-robust metallosupramolecular hydrogels with unprecedented self-recoverability using asymmetrically distributed carboxyl-Fe<sup>3+</sup> coordination interactions. *Chinese J. Polym. Sci.* 2023, 41, 250–257.

## INTRODUCTION

Hydrogels, polymer networks containing water as a solvent, have great potentials in various application, such as tissue engineering,<sup>[1,2]</sup> bioengineering,<sup>[3,4]</sup> wearable sensors<sup>[5,6]</sup> and enhanced oil recovery.<sup>[7,8]</sup> However, owing to permanent crosslinking and inhomogeneous network, the mechanical properties of the conventional hydrogels are relatively weak.<sup>[9,10]</sup> Natural load-bearing materials, such as cartilages and muscles, exhibit combinations of contradicting mechanical properties.<sup>[11,12]</sup> However, novel hydrogels with excellent mechanical performances can be devoted to resemble the comprehensive properties of the natural load-bearing tissues. This can be realized through different network topologies and energy dissipation mechanisms, such as in double-network,<sup>[13,14]</sup> slip-ring,<sup>[15]</sup> macromolecular-crosslinked,<sup>[10,16]</sup> microgel-reinforced,<sup>[17,18]</sup> and supramolecular hydrogels.<sup>[19–28]</sup>

Among these robust hydrogels, those based on supramolecular interactions with metal-coordination bonds have

attracted wide attraction owing to their high elastic modulus, good processability and recyclability, rapid stimulus responsiveness, and simple yet effective strengthening strategy. For instance, Suo *et al.*<sup>[29]</sup> designed the highly tough and stretchable hybrid hydrogels crosslinked *via* the coordination interactions between Ca<sup>2+</sup> and carboxyl groups of alginate, demonstrating 2300% ultimate strain and 74% recovery of hysteresis after one-day storage at 80 °C. Zhou *et al.*<sup>[21]</sup> developed a class of robust poly(acrylamide-co-acrylic acid) hydrogels comprising first chemical crosslinking with *N,N'*-methylenebisacrylamide (MBA) and second physical crosslinking through coordination bonds between Fe<sup>3+</sup> and carboxyl groups. These hydrogels exhibit a tensile strength of 6 MPa, strain at break of 700%, and hysteresis recovery of 87.6% after a 4 h resting period. Moreover, Wang *et al.*<sup>[27]</sup> applied the ion immersing method for forming imidazole-Cu<sup>2+</sup> complexes in the chemically crosslinked poly(acrylamide-co-vinylimidazole) hydrogel, enhancing its ultimate stress and strain to 7.7 MPa and 560%, respectively. Recently, Wu *et al.*<sup>[26]</sup> reported a facile approach for strengthening poly(acrylamide-co-2-acrylamido-2-methyl-1-propanesulfonic acid) hydrogels by forming sulfonate-Zr<sup>4+</sup> coordination complexes. These hydrogels showed remarkable mechanical performances with

\* Corresponding authors, E-mail: zhengjing@scu.edu.cn (J.Z.)

E-mail: wujinrong@scu.edu.cn (J.R.W.)

Received May 11, 2022; Accepted June 10, 2022; Published online August 31, 2022

stress up to 5.7 MPa and strain at break up to 1250%. After 20 min, the residual strain decreased to zero, and the recovery of hysteresis reached 85%. Despite such efforts, developing mechanically robust hydrogels is challenging to mimic the comprehensive mechanical properties of load-bearing tissues and achieve 100% recovery within seconds.

Herein, we present a robust hydrogel (tensile strength up to 12.5 MPa and Young's modulus up to 14 MPa) that can rapidly self-recover (achieve 99% of maximum toughness recovery for 300 s) at room temperature without any stimuli. The hydrogel is designed by combining two key strategies: (1) by introducing a special functional monomer containing two asymmetric carboxyl groups, itaconic acid (ITA), for copolymerizing with acrylamide; (2) by creating the Fe<sup>3+</sup>-carboxyl coordination bonds to form strong physical crosslinks and dissipate energy effectively. We believe such a simplified fabrication method illustrated in this study will provide a new platform to develop robust hydrogels with rapid self-recoverability.

## EXPERIMENTAL

### Materials

Itaconic anhydride (ITAH, 98%), *N,N'*-methylene-bis-acrylamide (MBA, 99%), potassium persulfate (KPS, 99.5%) and tetramethylethylenediamine (TMEDA, 99%) were obtained from Adamas, China. Acrylamide (AM, 99%), ferric (III) chloride hexahydrate (FeCl<sub>3</sub>·6H<sub>2</sub>O, 99%) and poly(ethylene glycol) (PEG, *M<sub>n</sub>*=20000) were received from Chengdu Huaxia Chemical Reagent Co., Ltd., China. Hydroxy silicone oil was imported from Wacker Chemical Co., Ltd., Germany. Deionized water was obtained from homemade in the laboratory.

### Preparation of Hydrogels

The typical poly(AM-co-ITA) hydrogels are fabricated by *in situ* free radical polymerization. Prescribed amounts of AM, ITAH, MBA and TMEDA are dissolved in deionized water. Ascribed to the hydrolysis of the anhydride, itaconic anhydride become itaconic acid when completely dissolved in water. After outgassing by a vacuum pump for 10 min, 180 mg/10g of KPS aqueous solution as initiator is added into the reaction solution. Next, the solution is transferred to a reaction box consisting of the organic glass mold and stored at 34 °C for 48 h. After thorough reaction, the samples are soaked in 0.1 mol/L FeCl<sub>3</sub> solution at room temperature for 10 h, thus forming pristine physical cross-linking networks. The above-obtained hydrogels are then immersed in overmuch deionized water for 24 h to remove excess Fe<sup>3+</sup> ions and optimize coordinates. At last, the hydrogels are placed in PEG aqueous solution (40 wt%) at room temperature and dehydrated slowly to about 45 wt% water content. The whole dehydrated process is spontaneous ascribed to the osmolarity, ensuring that the entire procedure is in a dynamic equilibrium.

### Characterizations

Fourier transform infrared spectroscopy in the mode of attenuated total reflection (ATR-FTIR, Nicolet 6700, Thermo Scientific, USA), Raman spectroscopy (HR Evolution, Horiba, Japan) and UV-Vis diffuse-reflectance spectrum (UV 3600, Shimadzu, Japan) are recorded to verify the formation of coordination interactions.

Rheological behaviors of the hydrogels are analyzed by a rotational rheometer (ARES G2, TA Instrument, USA) with a suit of 25 mm diameter parallel-plates. To keep hydrogels hydrated, the samples are smeared with a wafery layer of low-viscosity silicone oil during the testing. The frequency sweeps with variable temperature ranging from 10 °C to 60 °C are performed at an immobile strain of 0.1%. The spectra of storage modulus (*G'*), loss modulus (*G''*) are recorded, of which loss factor (tanδ) is the ratio of *G''* to *G'*. Master curves are acquired by time-temperature superposition displacement at a reference temperature of 10 °C. The apparent activation energies are calculated from the slope of the master curves according to Arrhenius' plot. Strain sweep is performed to the hydrogel samples from 0.01% to 100% at a frequency of 1 Hz at room temperature.

All the mechanical performances of the hydrogels are measured *via* a commercial tensile tester (5567, Instron, USA). The as-prepared dumbbell shape hydrogel samples for the uniaxial tensile test are tested at 100 mm/min at room temperature. Young's modulus is obtained from the initial slope of the stress-strain curve and the toughness is determined by the integral area of the stress-strain curve when the sample fracture.

The uniaxial tensile tests are also conducted at different stretch rates and temperatures to study the dynamic properties of these metallosupramolecular hydrogels. Immediately after the samples reach the thermal equilibrium by immersion in a water bath for 1 min at setting temperature, the hydrogels are tested for tensile strength. For the self-recovery measurement, the hydrogel is stretched to a vested length and then return to the original position at the same speed. Before the next loading procedure, the samples are kept in silicone oil to prevent water loss, resting for a certain period at room temperature. The recovery ratio is calculated by the ratio of the hysteresis area after each resting time to the original hysteresis loop. The residual strain ratio was defined as the ratio of the residual strain after each resting time to the original residual strain.

## RESULTS AND DISCUSSION

The robust metallosupramolecular hydrogels are fabricated *via* a three-step method, as illustrated in Fig. 1(a). The original poly(AM-co-ITA) hydrogels are synthesized by polymerizing the reaction solution containing AM, ITAH, and chemical crosslinkers (Table S1 in the electronic supplementary information, ESI). Thereafter, the hydrogels are incubated in 0.1 mol/L FeCl<sub>3</sub> solution for forming a physical crosslinking network and then immersed in excessive deionized water for removing the residuals and reaching the equilibrium state. Finally, the specimens are dehydrated to ~45% water content, eventually yielding the robust metallosupramolecular hydrogels (PAI-*f*-Fe<sup>3+</sup> gels, where *f* represents the mole percent of ITAH to total monomer). The resultant robust gels possess excellent load-bearing capacity, whereas the original uncoordinated hydrogels are friable and readily breakable upon small deformation (Fig. 1b). The diverse mechanical properties of hydrogels before and after the strengthening process (*i.e.*, coordination process) are investigated *via* uniaxial tensile tests (Fig. 1c and Fig. S1 in ESI). The original PAI-8 hydrogel consistent with the PAI-8-Fe<sup>3+</sup> water

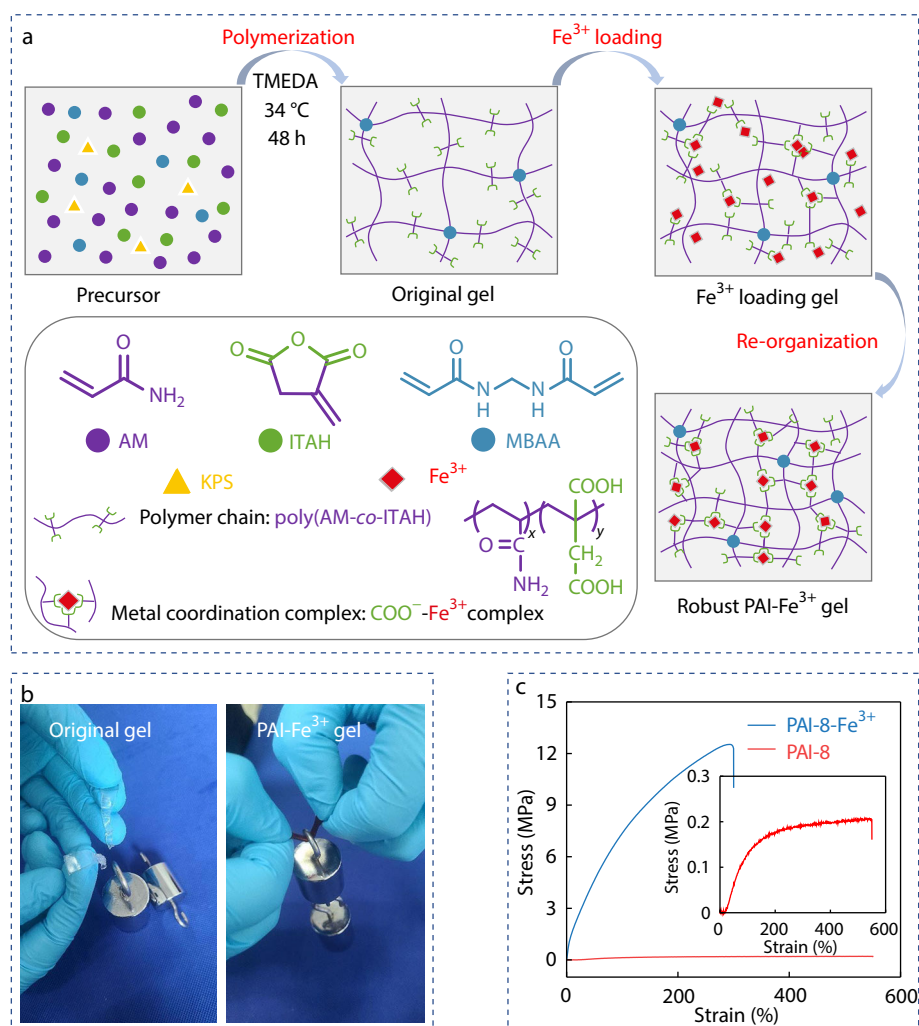


**Fig. 1** (a) Schematic illustration for the fabrication of PAI-Fe<sup>3+</sup> hydrogels; (b) Photos to demonstrate the weak of original PAI-8 hydrogel and robust PAI-8-Fe<sup>3+</sup> hydrogel; (c) Tensile stress-strain curves of the PAI-8-Fe<sup>3+</sup> hydrogel and PAI-8 hydrogel (with the same water content as PAI-8-Fe<sup>3+</sup>).

content is very weak, with ultimate stress of 0.20 MPa, Young's modulus of 0.15 MPa and toughness of 0.90 MJ/m<sup>3</sup>. These values remarkably increase to 12.5 MPa, 14.0 MPa and 25.5 MJ/m<sup>3</sup>, respectively, after being strengthened (corresponding to PAI-8-Fe<sup>3+</sup> gel). The original hydrogels can also be toughened by other metallic ions with robust binding strength, such as Cu<sup>2+</sup>, Cr<sup>3+</sup> and Zr<sup>4+</sup> ions (Fig. S2 in ESI). However, the Fe<sup>3+</sup>-carboxyl coordination complexes have the highest binding strength and stability for poly(AM-co-ITA) hydrogels.

The remarkable mechanical properties of the metallosupramolecular hydrogels are associated with the formation of the carboxyl-Fe<sup>3+</sup> coordination complexes, which is demonstrated by FTIR spectra (Fig. 2a). The bands at 1610 and 1660 cm<sup>-1</sup> on the FTIR spectra are assigned to the asymmetric stretching vibrations of carboxyl groups. The distinctions of these characteristic bands between PAI-8 and PAI-8-Fe<sup>3+</sup> gels indicates the formation of coordination complexes.<sup>[23,26]</sup> Furthermore, the Raman spectra clearly show the shift of the characteristic peaks of carboxyl groups from 1450 cm<sup>-1</sup> to 1454 cm<sup>-1</sup> and 1648 cm<sup>-1</sup> to 1660 cm<sup>-1</sup> (Fig. 2b), suggesting the formation of coordination bonds. Moreover, the forma-

tion of supramolecular network of the hydrogels can also be confirmed *via* UV-Vis spectra (Fig. 2c). When compared to the PAI-8 gel and Fe<sup>3+</sup> solution, the coordinated PAI-8-Fe<sup>3+</sup> gel shows a shoulder peak between 450 and 700 nm.

The mechanical properties of these robust metallosupramolecular hydrogels can be regulated over a wide range *via* controlling the molar content of ITAH (Table S2 in ESI). The total concentration of monomers and chemical crosslinkers is fixed at 4.5 mol/L and 0.07 mol% (relative to monomers), respectively. As shown in Figs. 3(a) and 3(b), as the ITAH/(ITAH+AM) monomer molar ratio (*f*) increases from 2% to 10.0%, the ultimate strain ( $\epsilon_b$ ) decreases from 842% to 249%, and the ultimate stress ( $\sigma_i$ ) as well as the modulus (*E*) initially increase and decrease, reaching a maximum value of 12.5 and 14.0 MPa at *f* of 8.0%, respectively. The toughness (*T*) measured by the area of the hysteresis loop fluctuates between 9.0 and 28.2 MJ/m<sup>3</sup>, which increases and then decreases with increasing *f*, exhibiting a maximum value of 28.2 MJ/m<sup>3</sup> at *f*=4.0%. Notably, when *f* exceeds 8%, the mechanical properties of the hydrogel decrease. The excess interfacial carboxyl groups and Fe<sup>3+</sup> ions form dense complexes on the

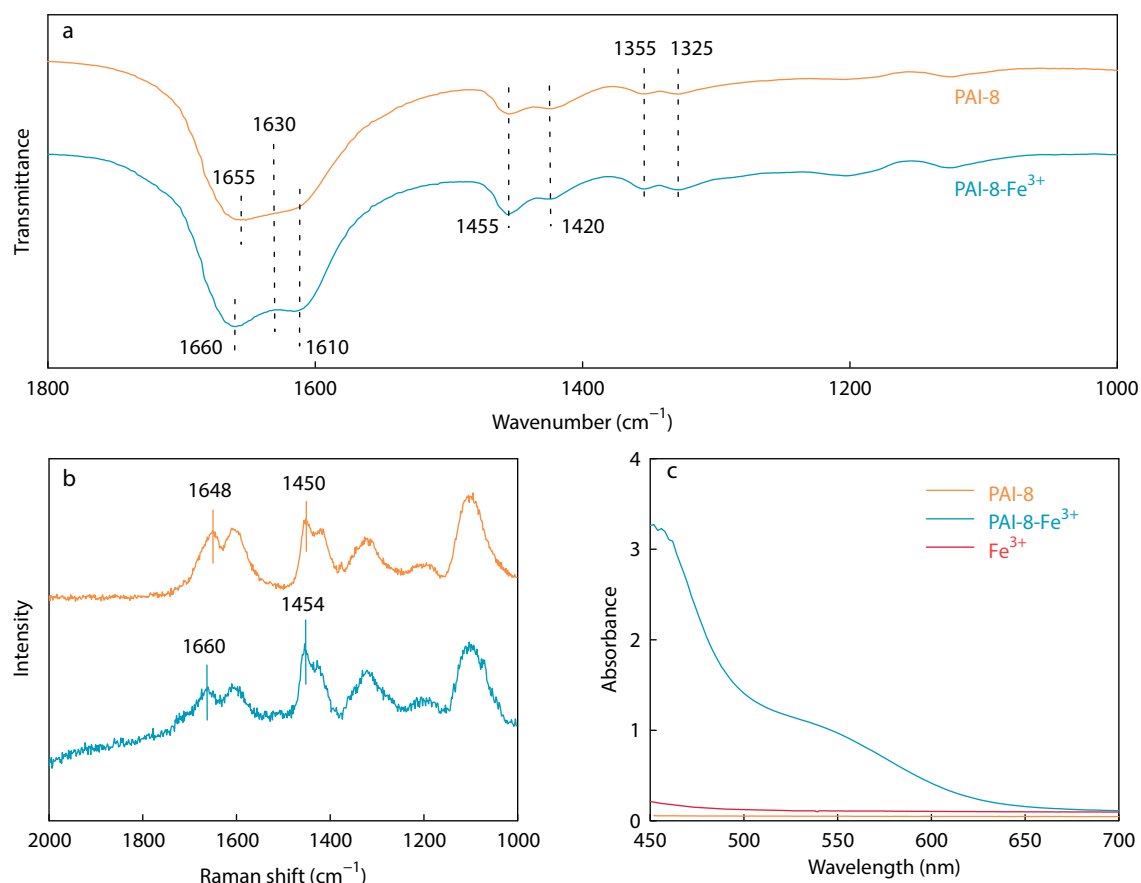


**Fig. 2** (a) FTIR spectra and (b) Raman spectra of the uncoordinated (PAI-8) and coordinated (PAI-8-Fe<sup>3+</sup>) hydrogels; (c) UV-Vis spectra of the uncoordinated (PAI-8), coordinated (PAI-8-Fe<sup>3+</sup>) hydrogels and FeCl<sub>3</sub> solution (0.1 mol/L).

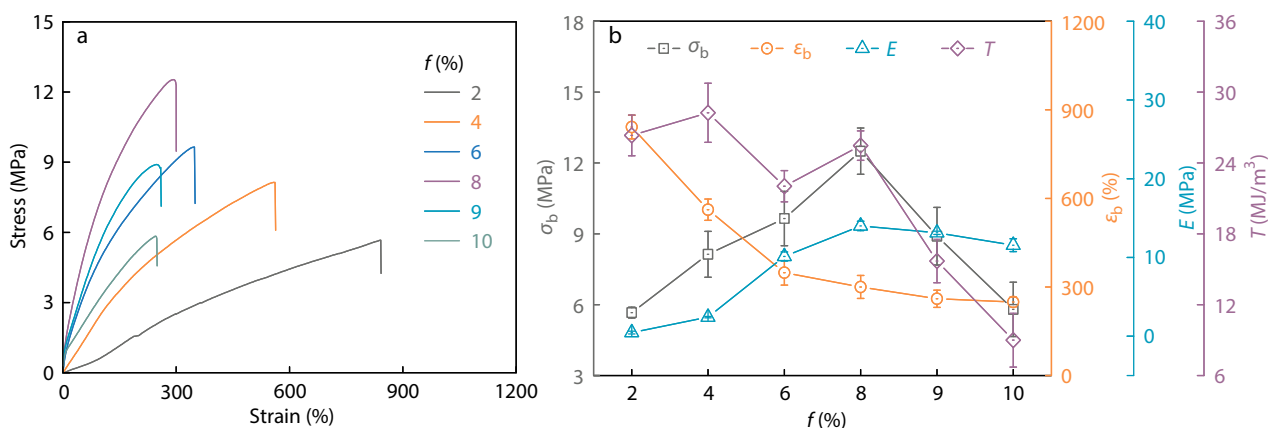


**Fig. 3** (a) Tensile stress-strain curves and (b) corresponding ultimate stress ( $\sigma_b$ ), ultimate strain ( $\epsilon_b$ ), modulus ( $E$ ) and toughness ( $T$ ) parameters of the PAI- $f$ -Fe<sup>3+</sup> hydrogels with different molar ratios of ITAH/ (ITAH + AM),  $f$ .

hydrogel surface, preventing the penetration of Fe<sup>3+</sup> ions into the hydrogel interior to participate in coordination. Overall, the robust metallosupramolecular hydrogels can be readily prepared with custom mechanical performances over a wide spectral range by adjusting the feeding  $f$ , which may facilitate utility applications.

Owing to the dynamic properties of the coordination network, the mechanical performances of the metallosupramolecular hydrogels depend on the stretch rate ( $v$ ) and tensile temperature ( $T$ ). When  $v$  increases from 1 mm/min to

500 mm/min,  $E$  and  $\sigma_b$  increase from 7.9 MPa and 9.5 MPa to 17.8 MPa and 14.2 MPa, respectively, and  $\epsilon_b$  decreases from 357% to 262% (Figs. 4a and 4b). The rate-dependent mechanical behavior is concerned with the dynamic time scale of coordination bonds, relative to the stretch rate. At a higher stretch rate, the coordination network can barely dissociate, causing a permanent physical crosslinking and deformation resistance, increasing  $E$  as well as  $\sigma_b$  and decreasing  $\epsilon_b$ .

Tensile temperature considerably affects the mechanical performance of hydrogels. Immediately after the hydrogel

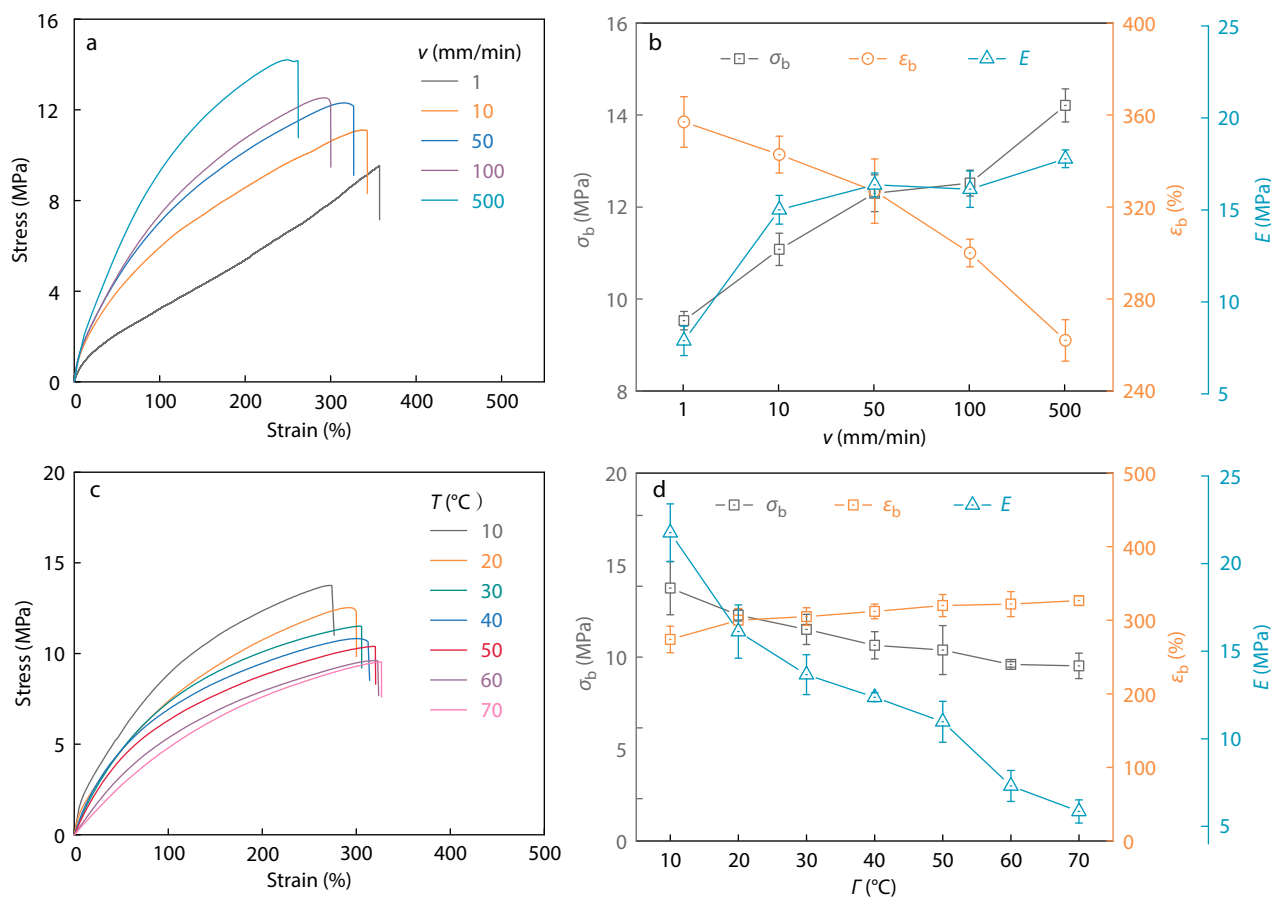


**Fig. 4** (a, c) Nominal stress-strain curves and (b, d) corresponding mechanical performance of the PAI-8-Fe<sup>3+</sup> hydrogel at different stretch rates (a, b) and different temperatures (c, d).

samples reach the thermal equilibrium instead of the swelling equilibrium by immersion in a water bath for 1 min at setting temperature, the hydrogels are performed for tensile strength. When  $T$  increases from 10 °C to 70 °C,  $E$  and  $\sigma_b$  decrease from 13.75 MPa and 21.76 MPa to 9.52 MPa and 5.85 MPa, respectively, and  $\varepsilon_b$  slightly increases from 274% to 327% (Figs. 4c and 4d). The temperature-dependent mechanical behavior can be attributed to the decrease in binding strength and stability of the coordination bonds at high temperatures. The temperature-dependent behavior of these metallosupramolecular hydrogels is investigated further by frequency sweeps at gradient temperatures. Figs. 5(a)–5(h) show that the master curves of the storage modulus ( $G'$ ), loss modulus ( $G''$ ) and loss factor ( $\tan\delta$ ) are constructed by the time-temperature superposition (TTS) of the frequency-dependent rheological curves. For all the hydrogels,  $G'$  decreases while  $G''$  increases with a decrease in frequency, demonstrating the gradual decomposition of coordination bonds with time. The shift factors ( $\ln a_T$ ) obtained by the TTS assist in realizing high apparent activation energy ( $E_a$ ) for each hydrogel, corresponding to the strong physical association. The values of  $E_a$  increase from 72.50 kJ/mol to 98.46 kJ/mol, with an increase in  $f$  from 2.0% to 8.0%, indicating that the increased ITA could increase the coordination density of hydrogel network and enhance their association

strength (Fig. 5i).

As previously mentioned, the hydrogels exhibit excellent dynamic nature and viscoelasticity, we expect they demonstrate good self-recoverability. A rheological strain sweep test is performed for determining the linear viscoelastic region (Fig. 6a). The  $G'$  and  $G''$  of PAI-8-Fe<sup>3+</sup> hydrogel remain fixed over a strain range from 0.005% to 0.2%. With increasing strain, the moduli exhibit an obvious reduction and  $G'$  intersects with  $G''$ , demonstrating the dissociation of dynamic coordination complexes. Furthermore, the successive step-shear measurements under different strains are performed. As shown in Fig. 6(b), the  $G'$  and  $G''$  of the hydrogel recover rapidly after decreasing the oscillation strain from 100% to 0.1%, suggesting the dynamic “dissociation-recombination” nature of coordination bonds under deformation. We performed the cyclic loading–unloading measurements on the hydrogels with different resting times to investigate their ability to recover upon loading macroscopically (Fig. 6c). After 100% stretching, the recovery ratio of hysteresis area and modulus with only one minute of resting reaches 94.5% and 87.7%, respectively. With increasing resting time to 5 minutes, the loading–unloading hysteresis loop practically overlaps with the original pathway, representing excellent self-recoverability (Fig. 6d). Large hysteresis is observed after reloading, demonstrating effective energy dissipation and that the hydrogel is not instantaneously resilient.<sup>[16]</sup> The rapid self-reco-



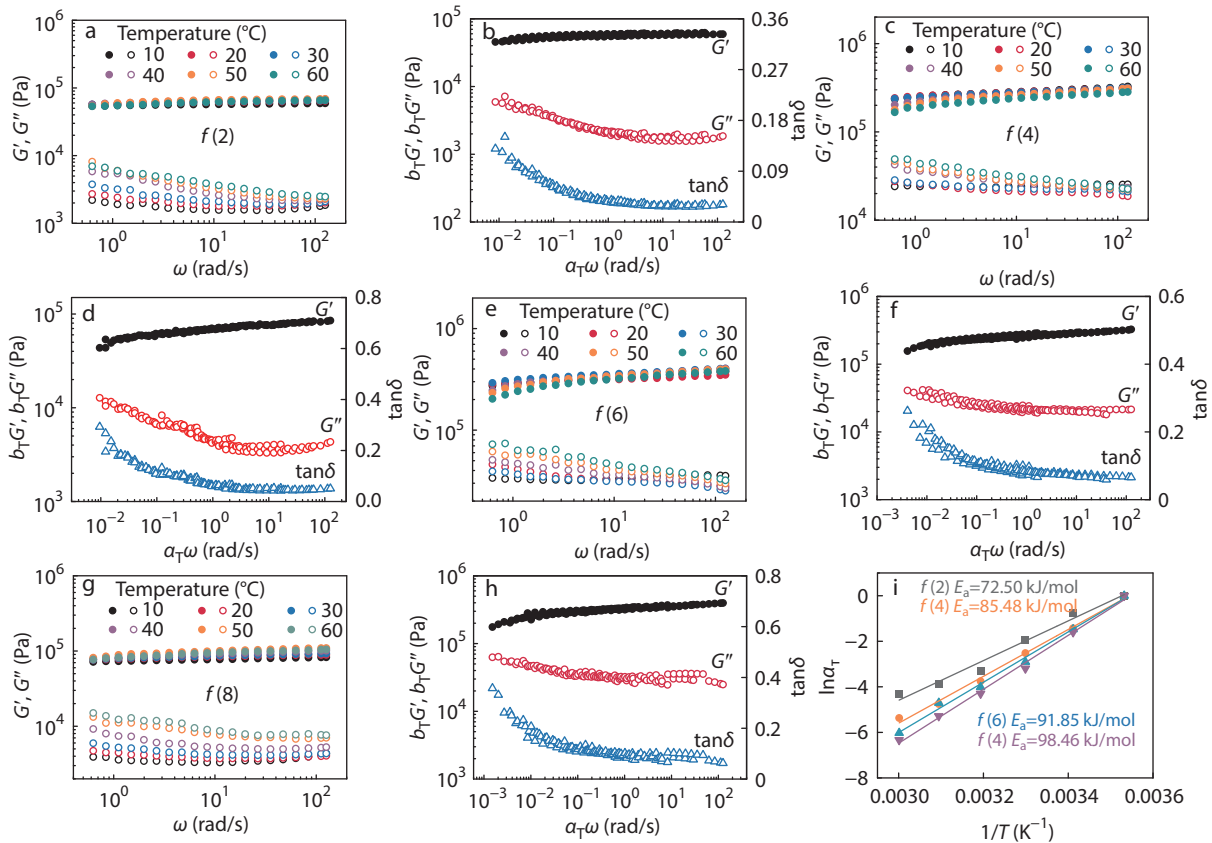


**Fig. 5** (a–h) Dynamic frequency sweeps with a temperature range of 10–60 °C of the PAI- $f$ -Fe $^{3+}$  hydrogels (a, c, e, g), the master curves acquired by shifting the frequency sweep curves at gradient temperatures (b, d, f, h); (i) Arrhenius plot of the aclinic shift factor  $\ln\alpha_T$  with a reference temperature of 10 °C.

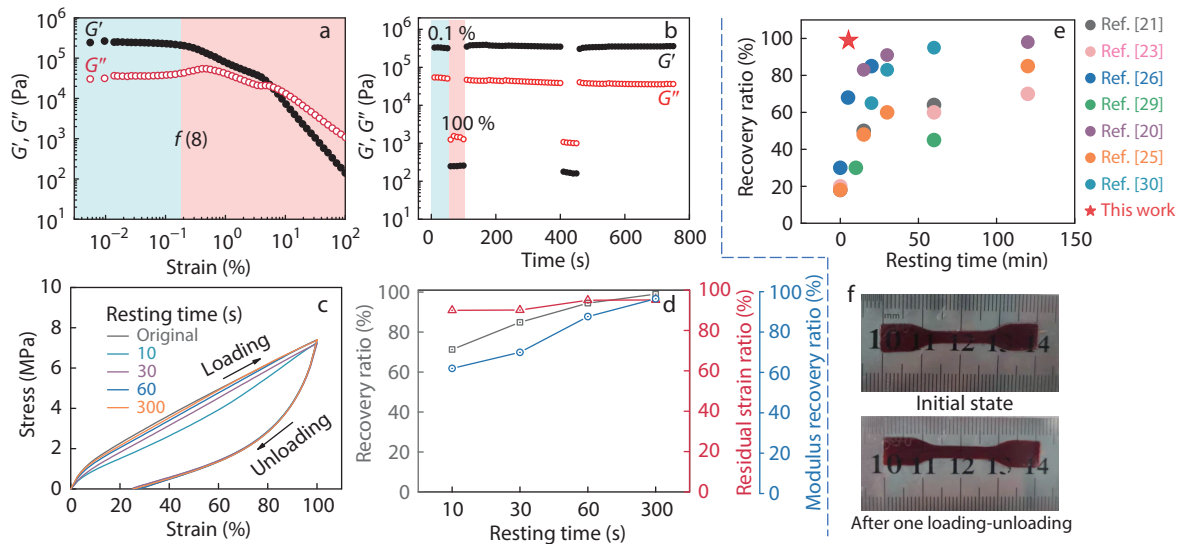


**Fig. 6** (a) The modulus ( $G'$  and  $G''$ ) versus strain-sweep curves of PAI-8-Fe $^{3+}$  hydrogel (frequency=1.0 Hz); (b) Modulus dependence on time in successive shear strain tests for PAI-8-Fe $^{3+}$  hydrogel with repeated small oscillation strain (strain=0.01%, frequency=1.0 Hz) and large oscillation strain (strain=50%, frequency=1.0 Hz); (c) Cyclic tensile curves at 100% strain with distinct waiting times between two continuous tests, and (d) the recovery ratio, residual strain ratio and modulus recovery ratio; (e) Material property charts of resting time versus recovery ratio for various reported supramolecular hydrogels, poly(acrylamide-co-acrylic acid-co- $N,N'$ -methylenebisacrylamide)-Fe $^{3+}$  gel,<sup>[21]</sup> poly(acrylamide-co-acrylic acid)-Fe $^{3+}$  gel,<sup>[23]</sup> poly(acrylamide-co-2-acrylamido-2-methyl-1-propanesulfonic acid)-Zr $^{4+}$  gel,<sup>[26]</sup> polyacrylamide-sodium alginate-Ca $^{2+}$  gel,<sup>[29]</sup> polyampholytes gel,<sup>[20]</sup> poly(acrylamide-co-maleic anhydride)-Fe $^{3+}$  gel,<sup>[25]</sup> polyacrylic acid-cellulose nanofibrils-Fe $^{3+}$  gel;<sup>[30]</sup> (f) Photos of the PAI-8-Fe $^{3+}$  hydrogel before (initial state) and after one loading–unloading tensile test.

very mechanism of these robust hydrogels can be summarized as follows: the permanent covalent crosslinked network; the unique topological network introduced by the asymmetric carboxyl groups. To demonstrate this, we prepare the physical hydrogels without MBA, which still exhibit a good recoverability-to-recovery ratio of hysteresis area up to 88% at 5 min rest (Fig. S3 in ESI). Overall, these hydrogels simultaneously possess outstanding self-recoverability, superior to most existing supramolecular hydrogels (Fig. 6e).<sup>[20,21,23,25,26,29,30]</sup> Furthermore, no considerable tissue damage and length change before and after one loading–unloading test (Fig. 6f) confirm the unexceptionable recovery performance of hydrogels.

## CONCLUSIONS

In summary, we have presented a facile strategy for fabricating ultra-robust hydrogels with unprecedented self-recoverability. The hydrogels are prepared by copolymerizing acrylamide and ITA in the presence of MBA, followed by physical crosslinking *via* coordination interactions. The strong yet asymmetrically distributed carboxyl-Fe<sup>3+</sup> complexes considerably increase the hydrogel's crosslinking density. The reversible dissociation-and-reorganization behavior effectively dissipate mechanical energy and redistribute stress concentration of hydrogels, affording their improved mechanical performance and excellent self-recoverability. Considering the developed asymmetrically distributed carboxyl groups in various polymer systems, the traditional metallosupramolecular hydrogels show rapid damage recovery.

## NOTES

The authors declare no competing financial interest.

## Electronic Supplementary Information

Electronic supplementary information (ESI) is available free of charge in the online version of this article at <http://doi.org/10.1007/s10118-022-2818-x>.

## ACKNOWLEDGMENTS

This work was financially supported by National Natural Science Foundation of China (No. 51873110).

## REFERENCES

- Gjorevski, N.; Nikolaev, M.; Brown, T. E.; Mitrofanova, O.; Brandenburg, N.; DelRio, F. W.; Yavitt, F. M.; Liberali, P.; Anseth, K. S.; Lutolf, M. P. Tissue geometry drives deterministic organoid patterning. *Science* **2022**, *375*, eaaw9021.
- Miao, S.; Castro, N.; Nowicki, M.; Xia, L.; Cui, H.; Zhou, X.; Zhu, W.; Lee, S. jun; Sarkar, K.; Vozzi, G.; Tabata, Y.; Fisher, J.; Zhang, L. G. 4D printing of polymeric materials for tissue and organ regeneration. *Mater. Today* **2017**, *20*, 577–591.
- Zhu, J.; Yang, S.; Qi, Y.; Gong, Z.; Zhang, H.; Liang, K.; Shen, P.; Huang, Y.; Zhang, Z.; Ye, W.; Yue, L.; Fan, S.; Shen, S.; Mikos, A. G.; Wang, X.; Fang, X. Stem cell-homing hydrogel-based miR-29b-5p delivery promotes cartilage regeneration by suppressing senescence in an osteoarthritis rat model. *Sci. Adv.* **2022**, *8*, eabk0011.
- Liang, Q.; Xia, X.; Sun, X.; Yu, D.; Huang, X.; Han, G.; Mugo, S. M.; Chen, W.; Zhang, Q. Highly stretchable hydrogels as wearable and implantable sensors for recording physiological and brain neural signals. *Adv. Sci.* **2022**, 2201059.
- Zhang, C.; Wang, M.; Jiang, C.; Zhu, P.; Sun, B.; Gao, Q.; Gao, C.; Liu, R. Highly adhesive and self-healing  $\gamma$ -PGA/PEDOT:PSS conductive hydrogels enabled by multiple hydrogen bonding for wearable electronics. *Nano Energy* **2022**, *95*, 106991.
- Zhuo, S.; Song, C.; Rong, Q.; Zhao, T.; Liu, M. Shape and stiffness memory ionogels with programmable pressure-resistance response. *Nat. Commun.* **2022**, *13*, 1743.
- Li, J.; Jiang, Z.; Wang, Y.; Zheng, J.; Huang, G. Stability, seepage and displacement characteristics of heterogeneous branched-preformed particle gels for enhanced oil recovery. *RSC Adv.* **2018**, *8*, 4881–4889.
- Yin, H.; Yin, X.; Cao, R.; Zeng, P.; Wang, J.; Wu, D.; Luo, X.; Zhu, Y.; Zheng, Z.; Feng, Y. *In situ* crosslinked weak gels with ultralong and tunable gelation times for improving oil recovery. *Chem. Eng. J.* **2021**, *432*, 134350.
- Kim, J.; Zhang, G.; Shi, M.; Suo, Z. Fracture, fatigue, and friction of polymers in which entanglements greatly outnumber cross-links. *Science* **2021**, *374*, 212–216.
- Cao, Z.; Wang, Y.; Wang, H.; Ma, C.; Li, H.; Zheng, J.; Wu, J.; Huang, G. Tough, ultrastretchable and tear-resistant hydrogels enabled by linear macro-cross-linker. *Polym. Chem.* **2019**, *10*, 3503–3513.
- Hua, M.; Wu, S.; Ma, Y.; Zhao, Y.; Chen, Z.; Frenkel, I.; Strzalka, J.; Zhou, H.; Zhu, X.; He, X. Strong tough hydrogels *via* the synergy of freeze-casting and salting out. *Nature* **2021**, *590*, 594–599.
- Liu, X.; Wu, J.; Qiao, K.; Liu, G.; Wang, Z.; Lu, T.; Suo, Z.; Hu, J. Topoarchitected polymer networks expand the space of material properties. *Nat. Commun.* **2022**, *13*, 1622.
- Gong, J. P.; Katsuyama, Y.; Kurokawa, T.; Osada, Y. Double-network hydrogels with extremely high mechanical strength. *Adv. Mater.* **2003**, *15*, 1155–1158.
- Gong, J. P. Why are double network hydrogels so tough. *Soft Matter* **2010**, *6*, 2583–2590.
- Liu, C.; Morimoto, N.; Jiang, L.; Kawahara, S.; Noritomi, T.; Yokoyama, H.; Mayumi, K.; Ito, K. Tough hydrogels with rapid self-reinforcement. *Science* **2021**, *372*, 1078–1081.
- Liu, R.; Wang, H.; Lu, W.; Cui, L.; Wang, S.; Wang, Y.; Chen, Q.; Guan, Y.; Zhang, Y. Highly tough, stretchable and resilient hydrogels strengthened with molecular springs and their application as a wearable, flexible sensor. *Chem. Eng. J.* **2021**, *415*, 128839.
- Hu, J.; Hiwatashi, K.; Kurokawa, T.; Liang, S. M.; Wu, Z. L.; Gong, J. P. Microgel-reinforced hydrogel films with high mechanical strength and their visible mesoscale fracture structure. *Macromolecules* **2011**, *44*, 7775–7781.
- Xia, L. W.; Xie, R.; Ju, X. J.; Wang, W.; Chen, Q.; Chu, L. Y. Nanostructured smart hydrogels with rapid response and high elasticity. *Nat. Commun.* **2013**, *4*, 1–11.
- Nan, W.; Wang, W.; Gao, H.; Liu, W. Fabrication of a shape memory hydrogel based on imidazole-zinc ion coordination for potential cell-encapsulating tubular scaffold application. *Soft Matter* **2013**, *9*, 132–137.
- Sun, T. L.; Kurokawa, T.; Kuroda, S.; Ihsan, A. Bin; Akasaki, T.; Sato, K.; Haque, M. A.; Nakajima, T.; Gong, J. P. Physical hydrogels composed of polyampholytes demonstrate high toughness and viscoelasticity. *Nat. Mater.* **2013**, *12*, 932–937.
- Lin, P.; Ma, S.; Wang, X.; Zhou, F. Molecularly engineered dual-crosslinked hydrogel with ultrahigh mechanical strength, toughness, and good self-recovery. *Adv. Mater.* **2015**, *27*, 2054–2059.
- Hu, Y.; Du, Z.; Deng, X.; Wang, T.; Yang, Z.; Zhou, W.; Wang, C. Dual physically cross-linked hydrogels with high stretchability, toughness, and good self-recoverability. *Macromolecules* **2016**, *49*, 5660–5668.

- 23 Zheng, S. Y.; Ding, H.; Qian, J.; Yin, J.; Wu, Z. L.; Song, Y.; Zheng, Q. Metal-coordination complexes mediated physical hydrogels with high toughness, stick-slip tearing behavior, and good processability. *Macromolecules* **2016**, *49*, 9637–9646.
- 24 Cao, J.; Li, J.; Chen, Y.; Zhang, L.; Zhou, J. Dual physical crosslinking strategy to construct moldable hydrogels with ultrahigh strength and toughness. *Adv. Funct. Mater.* **2018**, *28*, 1800739.
- 25 Ma, C.; Wang, Y.; Jiang, Z.; Cao, Z.; Yu, H.; Huang, G.; Wu, Q.; Ling, F.; Zhuang, Z.; Wang, H.; Zheng, J.; Wu, J. Wide-range linear viscoelastic hydrogels with high mechanical properties and their applications in quantifiable stress-strain sensors. *Chem. Eng. J.* **2020**, *399*, 125697.
- 26 Yu, H. C.; Zheng, S. Y.; Fang, L.; Ying, Z.; Du, M.; Wang, J.; Ren, K. F.; Wu, Z. L.; Zheng, Q. Reversibly transforming a highly swollen polyelectrolyte hydrogel to an extremely tough one and its application as a tubular grasper. *Adv. Mater.* **2020**, *32*, 2005171.
- 27 Jiao, C.; Zhang, J.; Liu, T.; Peng, X.; Wang, H. Mechanically strong, tough, and shape deformable poly(acrylamide-co-vinylimidazole) hydrogels based on Cu<sup>2+</sup> complexation. *ACS Appl. Mater. Interfaces* **2020**, *12*, 44205–44214.
- 28 Yu, H. C.; Hao, X. P.; Zhang, C. W.; Zheng, S. Y.; Du, M.; Liang, S.; Wu, Z. L.; Zheng, Q. Engineering tough metallosupramolecular hydrogel films with kirigami structures for compliant soft electronics. *Small* **2021**, *17*, 2103836.
- 29 Sun, J. Y.; Zhao, X.; Illeperuma, W. R. K.; Chaudhuri, O.; Oh, K. H.; Mooney, D. J.; Vlassak, J. J.; Suo, Z. Highly stretchable and tough hydrogels. *Nature* **2012**, *489*, 133–136.
- 30 Shao, C.; Chang, H.; Wang, M.; Xu, F.; Yang, J. High-strength, tough, and self-healing nanocomposite physical hydrogels based on the synergistic effects of dynamic hydrogen bond and dual coordination bonds. *ACS Appl. Mater. Interfaces* **2017**, *9*, 28305–28318.